

Revealing the footprints of squark gluino production through Higgs search experiments at the Large Hadron Collider at 7 TeV and 14 TeV

Biplob Bhattacharjee^{(a)1} and Amitava Datta^{(b)2}

^(a) *Department of Theoretical Physics, Tata Institute of Fundamental Research,
1, Homi Bhabha Road, Mumbai 400 005, India.*

^(b) *Indian Institute of Science Education and Research, Kolkata,
Mohanpur Campus, PO: BCKV Campus Main Office,
Mohanpur - 741252, India.*

Abstract

The invariant mass distribution of the di-photons from the decay of the lighter scalar Higgs boson(h) to be carefully measured by dedicated h search experiments at the LHC may be distorted by the di-photons associated with the squark-gluino events with much larger cross sections in Gauge Mediated Supersymmetry Breaking (GMSB) models. This distortion if observed by the experiments at the Large Hadron Collider at 7 TeV or 14 TeV, would disfavour not only the standard model but various two Higgs doublet models with comparable h - masses and couplings but without a sector consisting of new heavy particles decaying into photons. The minimal GMSB (mGMSB) model constrained by the mass bound on h from LEP and that on the lightest neutralino from the Tevatron, produce negligible effects. But in the currently popular general GMSB(GGMSB) models the tail of the above distribution may show statistically significant excess of events even in the early stages of the LHC experiments with integrated luminosity insufficient for the discovery of h. We illustrate the above points by introducing several benchmark points in various GMSB models - minimal as well as non-minimal. The same conclusion follows from a detailed parameter scan in a simplified GGMSB model recently employed by the CMS collaboration to interpret their searches in the di-photon + E_T channel. Other observables like the effective mass distribution of the di-photon + X events may also reveal the presence of new heavy particles beyond the Higgs sector. The contamination of the h mass peak and simple remedies are also discussed.

PACS no: 14.80.Da, 12.60.Jv

¹biplob@theory.tifr.res.in

²adatta@iiserkol.ac.in

1 Introduction

The search for the Higgs boson/bosons and the study of their properties tops the priority list of the on going experiments at the LHC at 7 TeV as well as of the upcoming experiments at the highest attainable energy of 14 TeV. This will shed light on the mechanism of electroweak symmetry breaking (EWSB) and the generation of the particle masses. The Higgs sector of the very successful standard model (SM) of particle physics responsible for EWSB is indeed very simple. It consists of a single neutral, scalar Higgs particle. However, this economical Higgs sector turns out to be the Achilles' heel of the SM.

The scale of EWSB is expected to be around 100 GeV. On the other hand the naturalness or the hierarchy problem [1, 2] comes into play, should there be some new physics beyond the SM characterized by a much higher energy scale. The very existence of the new scale tends to push up the EWSB scale far beyond the expected magnitude. For example, the Higgs boson mass blows up to values closer to the new scale, in contrast to the preferred range [3] $m_h = 89_{-26}^{+35}$ suggested by EW precision data (the hierarchy problem), unless the parameters of the SM are extremely fine tuned (the naturalness problem). Even the absence of any compelling evidence in favour of a new physics model does not allow us to overlook the above issues, since one cannot wish away the Planck scale, the scale of gravity which is always there.

The above theoretical inconsistency has led to several extensions of the SM. The minimal supersymmetric standard model(MSSM) [4] removes the above problem elegantly in the limit of exact supersymmetry (SUSY) and stabilizes the Higgs mass. However, SUSY must be broken by the soft breaking terms, since the negative results of sparticle searches at various colliders indicate that the superpartners (or the sparticles) must be considerably heavier than the corresponding particles. In spite of SUSY breaking, the naturalness problem remain under control, provided the masses of the sparticles are ~ 1 TeV [4] or smaller.

In the MSSM the Higgs sector must necessarily be extended and the spectrum consists of two neutral scalars (h and H), one neutral pseudo scalar (A) and two charged scalars (H^\pm) [4, 5]. Enormous amount of work has been done in developing the strategies for searching these bosons at the LHC [6, 7]. Adding any new dimension to the above studies is not the aim of this paper.

However, at the LHC these Higgs bosons are likely be produced along with a variety of superpartners of the standard model particles - the sparticles. In particular the strongly interacting sparticles may indeed be produced in numbers much larger than that of typical Higgs induced events. Even if a small fraction of such events pass through the selection criteria for the dedicated search of any of the above Higgs bosons, then the shape of certain distributions expected for Higgs production alone may change significantly, indicating that the Higgs boson may be part of a framework larger than the SM. Such an unexpected shape is likely to be prominent near the tails of the distributions under study where contributions from the Higgs signal as well as the SM background are naturally small. In this paper we shall illustrate this possibility with a specific example.

Some of the above issues have recently been addressed in the context of charged Higgs search by a counting experiment during the LHC-14 TeV run [8]. It has been demonstrated that both in the unconstrained MSSM and in the minimal supergravity(mSUGRA) model [9], SUSY events can seriously affect the size of the charged Higgs signal unless additional selection criteria are introduced. On the other hand, the combined squark-gluino and charged Higgs events may establish physics beyond the standard model (BSM) physics at a confidence level higher than that attainable by the Higgs signal alone. This enhancement would disfavour not only the SM but also its extensions with two Higgs doublets. After this important hint regarding BSM physics, a clean charged Higgs sample may be recovered by additional kinematical cuts. It needs to be emphasized that the above issues are relevant in any extension of the SM with a new particle sector as well as an extended Higgs sector.

In this paper we focus our attention on the search for the lighter CP even scalar Higgs boson(h). The h boson in the MSSM has properties very similar to the SM Higgs boson in a large volume of the parameter space (the so called decoupling region). Thus the discovery of a single neutral Higgs scalar, which is a likely scenario in the early stages of the LHC experiment, will yield very little information regarding the underlying theory. The situation may change dramatically if SUSY is realized in nature in such a way that a sizable number of sparticle induced events change the characteristics of the expected h signal significantly. This can convincingly establish the BSM origin of the discovered boson. Even the discovery of one or more heavier Higgs boson with no counterpart in the SM, would indicate only an extended Higgs sector but not the existence of new heavy sparticles.

The mass of h is always bounded from above ($m_h \leq 140$ GeV) [4] in supersymmetric theories. As a consequence the search strategy for it is very similar to that for the standard Higgs boson with mass within the above bound especially in the decoupling region. If $m_h < 130$ GeV, an important discovery channel would be the inclusive di-photon + X channel with a relatively modest integrated luminosity (\mathcal{L}) of a few tens of fb^{-1} at the 14 TeV run of the LHC (see Figure 10.38 of [6]). Here X stands for any other particle accompanying the h signal. This signal stems from h production at the LHC via several channels, followed by the one loop decay $h \rightarrow \gamma\gamma$. The suppression of the signal due to the tiny branching ratio (BR) of this decay ($\sim 10^{-3}$) is adequately compensated by the relatively low SM background. In the MSSM also a small peak in the $\gamma\gamma$ invariant mass distribution around the h mass would establish the h signal (see Figure 11.37 of [6]).

Among various models of softly broken supersymmetry the Gauge Mediated Supersymmetry Breaking (GMSB) models [10, 11] (to be briefly reviewed below) predict a large number of di-photon + X events at LHC energies coming from the production of strongly interacting sparticles. In this paper we wish to focus on the impact of these events on the di-photon invariant mass distribution to be studied by the dedicated h-search experiments with utmost care.

In these models the gravitino with negligible mass turns out to be the lightest supersymmetric particle (LSP) and, hence, the carrier of missing energy. If the lightest neutralino ($\tilde{\chi}_1^0$) is the next lightest supersymmetric

particle (NLSP), it can decay into the LSP and a photon with a large BR. In R-parity conserving supersymmetry, sparticles are produced in pairs and each of them eventually decay, through a cascade, into a gravitino-photon pair. Each SUSY event in this scenario will, therefore, have the $2\gamma + X$ topology. Thus the pair production of squarks and gluinos in any combination having a large cross section may leave their signature in the observed $\gamma\gamma$ invariant mass distribution.

The Plan of the paper is as follows. In the next section we briefly describe different GMSB scenarios and the present collider constraints on them. We also define our benchmark points for the analysis. In section 3, we present our main results on the di-photon invariant mass distribution in GMSB models at the LHC. Our emphasis will be on the ongoing LHC experiments. However, the possibilities for the 14 TeV experiments will also be briefly touched upon. Our conclusions will be summarized in section 4.

2 Different GMSB scenarios, sparticle spectra and the current collider constraints

To begin with we shall review the constraints from different collider experiments on the parameter space of the minimal GMSB (mGMSB) model [10, 11]. We also wish to add a few points regarding the approximations in obtaining these bounds and the resulting uncertainties which have not been sufficiently elucidated in the current literature. In this model the soft breaking parameters are generated via the gauge interactions of the SM. As a result the sparticles with the same SM quantum numbers but different flavours acquire the same mass. This keeps the potentially dangerous flavour changing neutral current induced processes under control.

In the mGMSB model there is an observable sector consisting of the MSSM fields. The supersymmetry breaking sector consists of a gauge singlet chiral superfield Y , identified with the goldstino superfield in the simplest version of the model. The scalar and auxiliary components of Y are assumed to develop vacuum expectation values (VEVs) denoted by S and F respectively. In the early versions of this model the dynamics of generating these VEVs were not specified. The model also has a messenger sector consisting of superfields Φ_i having the gauge interaction of the SM. The messenger superfields interact with Y via a tree level interaction in the superpotential. This generates a supersymmetric mass of $\mathcal{O}(M)$ of the messenger fields, usually referred to as the messenger scale. A SUSY breaking mass squared splittings of the order F is also generated within the messenger supermultiplets. This SUSY breaking is communicated to the observable sector by gauge interactions between the messenger and the observable fields via higher order processes. A restriction in the messenger sector comes from the requirement of the unification of the coupling constants of the standard model. If the messenger superfields form complete GUT multiplets (e.g., 5 or $\bar{5}$ of $SU(5)$), the value of the unification scale or the GUT scale (M_G) does not change. However, coupling constant unification constrains the number of messenger

superfields(N) to be ≤ 5 .

The simple mGMSB model is characterized by five parameters [10, 11]

$$\Lambda, M, N, \tan \beta \text{ and } \text{sign}(\mu)$$

where $\Lambda = F / S$ is the SUSY breaking scale in the observable sector, M is the messenger mass scale, N is the number of messenger multiplets belonging to the $5 + \bar{5}$ representation of $SU(5)$, $\tan \beta$ is the ratio of the vacuum expectation values of the neutral Higgs fields in the observable sector and μ is the Higgs mixing parameter in the superpotential with magnitude fixed by the radiative symmetry breaking condition. It bears recall that the soft breaking trilinear (A) and bilinear (B) parameters are generated by higher order processes and are small at the messenger scale M . The weak scale parameters are then obtained by the standard renormalization group (RG) evolutions. The sparticle spectrum at the weak scale can be computed by both SUSPECT version 2.41 [12] and ISAJET [13]. The phenomenology of this model has been discussed by various authors [14]

The current experimental lower bound on the Higgs boson mass from LEP $m_h > 114.4$ GeV [15] poses the strongest constraint on the parameter space of the mGMSB model. Given the input parameters one can compute the Higgs mass including higher order corrections. In this paper $m_h > 114.4$ GeV will be henceforth referred to as the stronger bound on the computed h-mass. However, there is an estimated theoretical uncertainty of about 3 GeV on the computed h-mass due to yet unknown higher order effects[16]. In view of this a point in the parameter space with computed $m_h \geq 111.4$ GeV (the weaker h-mass bound) may still be acceptable.

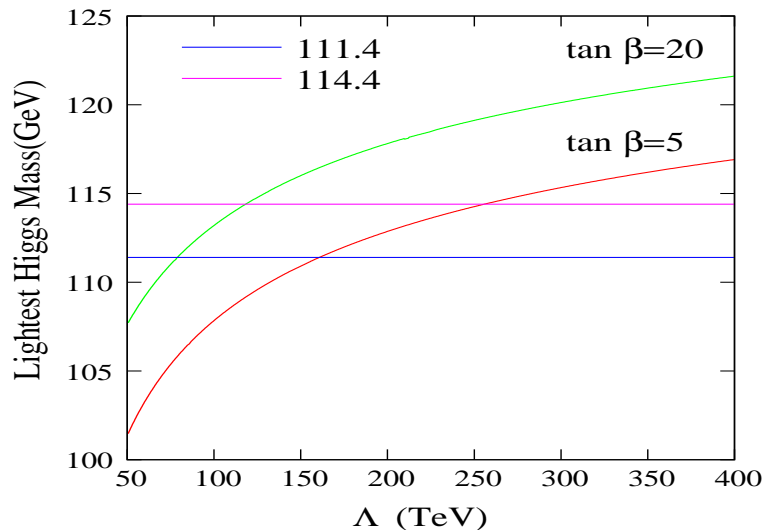


Figure 1: Variation of the computed Higgs mass with the SUSY breaking scale Λ (in TeV) for different $\tan \beta = 5$ (red line) and 20 (blue line) in the mGMSB model. No significant enhancement of the Higgs mass in the region $\tan \beta = 20$ to 50 has been noticed. The horizontal lines correspond to the Higgs mass 111.4 GeV and 114.4 GeV respectively. The top quark mass is fixed at 173 GeV and $M = 2 \Lambda$.

In Figure 1 we present m_h computed as a function of Λ . We take $m_t=173$ GeV, $M=2\Lambda$, $N=1$. It follows that for $\tan \beta = 5$ ($\tan \beta = 20$) the stronger h-mass bound yields a lower bound $\Lambda_{min} \geq 257$ TeV (118 TeV). If, however, the theoretical uncertainties are taken into account and the weaker m_h bound is used instead, relaxed bounds $\Lambda_{min} \geq 161$ TeV (79 TeV) are obtained. It is interesting to note that for $m_h \approx 120$, $\Lambda \approx 300$ GeV which corresponds to gluino mass ($m_{\tilde{g}}$) and average squark mass (m_0) of approximately 2 TeV and 3 TeV respectively. Thus should the Higgs mass bound continues to be pushed upwards, the squark-gluino search at the LHC, as predicted by mGMSB, will be quite challenging.

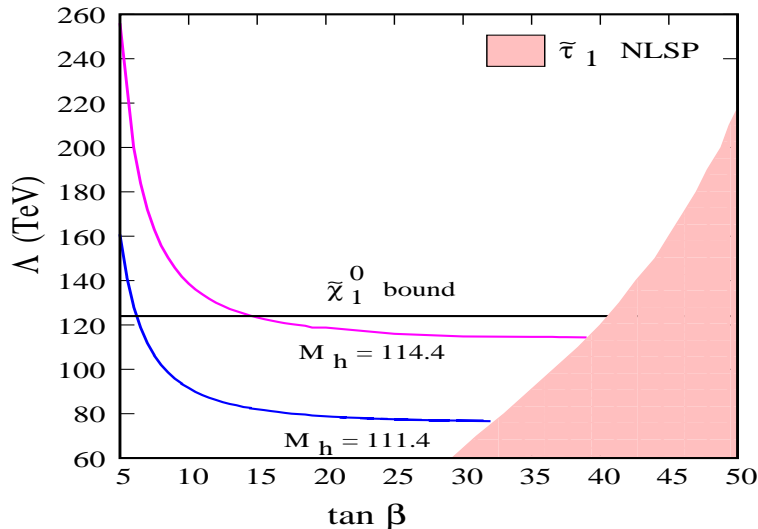


Figure 2: Allowed parameter space in the mGMSB model in the Λ (in TeV)- $\tan\beta$ plane. The other parameters are as in Figure 1. In the shaded (pink) region, $\tilde{\tau}_1$ is the NLSP. The magenta and blue lines correspond to the Higgs mass 114.4 GeV and 111.4 GeV respectively. The horizontal black line indicates the latest neutralino mass bound set by $D\mathcal{O}$ collaboration.

The $D\mathcal{O}$ and CDF collaborations have put strong constraints on NLSP (χ_1^0) mass. In order to obtain quantitative results they consider SPS8 slope in the mGMSB model which has only one parameter Λ . The other parameters are fixed and given by $M=2\Lambda$, $\tan\beta=15$, $N=1$ and $\mu > 0$. The lifetime of the χ_1^0 is not fixed by these parameters and it is assumed to be sufficiently short. It means that the photon coming from the decay of χ_1^0 is prompt. The gaugino pair production processes are expected to be dominant at the Tevatron. The decay of two χ_1^0 produce two photons and gravitinos that give rise to missing energy.

The latest constraint is from $D\mathcal{O}$ collaboration who have obtained a lower bound 124 TeV on the scale Λ with 6.3 fb^{-1} of data at Run II [17]. We have computed the leading order (LO) cross sections for the dominant SUSY processes at Tevatron energies (mainly electroweak gaugino pair production) using PYTHIA [18]. The next to leading order(NLO) cross section and the K factor with renormalization scale(μ_R)= factorization scale (μ_F)= $2m_{\tilde{\chi}_1^\pm}$ is computed by PROSPINO [19, 20]. Our cross section for $\Lambda=124$ TeV (assuming SPS8 point) is in good agreement with the result in [17]. We find that the above bound corresponds to an upper bound on the SUSY

production cross section of 4.5 fb. For promptly decaying $\tilde{\chi}_1^0$ this Λ_{min} yields $m_{\tilde{\chi}_1^0} \geq 174$ GeV. This bound is indicated in the $\Lambda - \tan\beta$ plane (Figure 2) by the horizontal line. For comparison the stronger and weaker h -mass bounds are also indicated in the same figure. It follows that the D0 bound on Λ_{min} supersedes that from the stronger (relaxed) m_h bound for $\tan\beta \gtrsim 15$ (6.5). It follows that irrespective of the uncertainties in m_h due to higher order corrections and the choice of $\tan\beta$, values of Λ smaller than 124 TeV are disfavoured. This bound also supersedes the earlier CDF lower bound on SUSY scale 107 TeV[21]. The assumptions underlying this bound will be critically examined below.

Strictly speaking the $D\tilde{\chi}$ bound is valid for the snowmass slope SPS8 with variable Λ . The other parameters are $M = 2\Lambda$, $N = 1$, $\tan\beta = 15$ and $\text{sign}(\mu) > 0$. For $N \geq 2$, the scenario reduces to a $\tilde{\tau}$ NLSP scenario which is not under consideration in the present paper.

However, keeping other parameters fixed and varying $\tan\beta$ we have checked that neither the cross sections of the dominant processes ($\tilde{\chi}_1^+ - \tilde{\chi}_2^0$ and $\tilde{\chi}_1^+ - \tilde{\chi}_1^-$ pair production [17, 21]) at the Tevatron energy nor the $\tilde{\chi}^+$ and $\tilde{\chi}_2^0$ masses vary appreciably with $\tan\beta$. This is, however, expected since over the scanned parameter space the above gauginos are wino like to a very good approximation and have masses controlled by the $SU(2)$ Gaugino mass M_2 at the weak scale. The cross section, therefore, shows only a mild $\tan\beta$ dependence.

The bino-like $\tilde{\chi}_1^0$ mass on the other hand is determined by the $U(1)$ gaugino mass parameter (M_1) at the weak scale related to M_2 by the gaugino mass unification condition. We shall, therefore, use the $D\tilde{\chi}$ bound throughout this analysis unless the electroweak gauginos happen to be significantly mixed, which is often the case for non-minimal models to be discussed below.

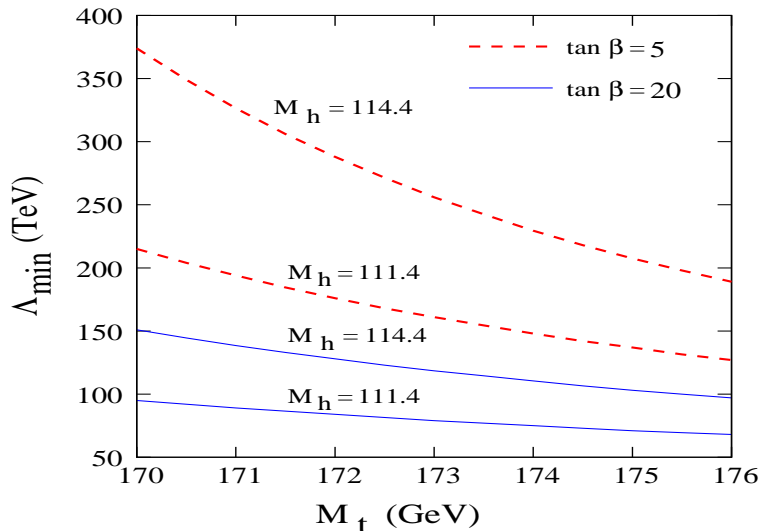


Figure 3: Minimum allowed value of the SUSY scale Λ as a function of the top mass obtained from the stronger and weaker Higgs mass bound for two values of $\tan\beta$.

The neutralino mass bound from Tevatron has an important advantage. The predicted m_h depends sensitively

Masses	CASE I	CASE II	CASE III
	$\tan\beta=20$	$\tan\beta=20$	$\tan\beta=20$
	$\Lambda=120$	$\Lambda=120$	$\Lambda=120$
	$M_m=2\Lambda$	$M_m=5\Lambda$	$M_m=10\Lambda$
$m_{\tilde{g}}$	997.6	963.8	959.1
$m_{\tilde{u}_L}$	1320.4	1293.6	1280.3
$m_{\tilde{u}_R}$	1264.4	1235.8	1221.2
$m_{\tilde{\nu}_e}$	417.4	420.3	423.6
$m_{\tilde{e}_L}$	424.6	427.5	430.8
$m_{\tilde{e}_R}$	209.7	213.3	216.4
$m_{\tilde{\tau}_1}$	199.9	202.2	204.6
$m_{\tilde{\chi}_1^0}$	169.1	162.8	161.9
$m_{\tilde{\chi}_2^0}$	321.4	311.8	311.1
$m_{\tilde{\chi}_1^\pm}$	321.1	311.7	310.9
m_h	114.5	114.3	114.1

Table 1: Variation of sparticle masses as a function of the Messenger scale (M_m) for fixed SUSY scale and $\tan\beta$ in the minimal GMSB model.

on m_t (recall the m_t^4 dependence in the radiative corrections to m_h). The minimum value of Λ consistent with the weaker or stronger h-mass bound as a function of m_t is presented in Figure 3 for two values of $\tan\beta$: 5 and 20. The top masses on the X-axis are allowed by the current bound obtained by a recent CDF measurement $m_t = 173.13 \pm 1.2$ [22].

These curves illustrate the uncertainty in Λ_{min} due to the present error in m_t . The neutralino mass bound, on the other hand, shows no strong m_t -dependence. Throughout this paper we shall use $m_t = 173$ GeV.

In summary, while choosing the representative points for calculating the SUSY contribution to the di-photon invariant mass spectrum in the GMSB model, the Λ_{min} from the weaker h-mass bound (neutralino mass bound) should be used for $\tan \lesssim 6.5$ ($\tan > 6.5$).

Another theoretical uncertainty comes from the choice of the messenger scale M . In Table 1 we present the variation of the sparticle spectrum with M . We find that the variation of M within moderate ranges does not affect the spectrum and, hence, the collider signatures drastically.

It should be emphasized that the CDF and $D\phi$ experiments actually constrain the quantity $\sigma_{SUSY} \times BR(\tilde{\chi}_1^0 \rightarrow \gamma \tilde{G})^2$, where σ_{SUSY} is the total sparticle production cross section within the kinematic reach of the Tevatron, $BR(\tilde{\chi}_1^0 \rightarrow \gamma \tilde{G})$ is the branching ratio underlying each single photon event. The cross section limit quoted above is, therefore, subject to the model dependent assumption $BR(\tilde{\chi}_1^0 \rightarrow \gamma \tilde{G})^2 \approx 1$.

The above BR depends on the neutralino mixing angles and may differ significantly from 1, if the lightest neutralino is indeed an admixture of electroweak gauginos and higgsinos. The widths of the different decay

$\Lambda(\text{TeV})$	BR ($\tilde{\chi}_1^0 \rightarrow \gamma \tilde{G}$)
105	0.950
125	0.907
145	0.874
165	0.849

Table 2: Branching fraction of $\tilde{\chi}_1^0 \rightarrow \gamma \tilde{G}$ for $\tan \beta=20$ and $M = 2\Lambda$ in the mGMSB model.

channels of $\tilde{\chi}_1^0$ are given, e.g., in Eqs 3.7 - 3.12 of [11]. The relative width of the $\tilde{\chi}_1^0$ decay into γ and Z is given by (following the notation of [11])

$$\Gamma(\tilde{\chi}_1^0 \rightarrow Z \tilde{G}) = (\kappa_Z / \kappa_\gamma)^2 \Gamma(\tilde{\chi}_1^0 \rightarrow \gamma \tilde{G}) \times (1 - (m_Z/m_{\tilde{\chi}_1^0})^2)^2$$

As long as the $\tilde{\chi}_1^0$ is a pure Bino, which is almost always the case in mGMSB, the ratio $(\kappa_Z / \kappa_\gamma)^2 \approx \tan^2 \theta_W$. Moreover for relatively small Λ , $m_{\tilde{\chi}_1^0} \approx m_Z$, and the Z-channel is strongly suppressed compared to the γ channel. However, as Λ and $m_{\tilde{\chi}_1^0}$ increases, the relative importance of the Z-channel increases even in the mGMSB model, due to the factor $(1 - (m_Z/m_{\tilde{\chi}_1^0})^2)^2$. As a result the BR ($\tilde{\chi}_1^0 \rightarrow \gamma \tilde{G}$) becomes significantly smaller than one. This is illustrated in Table 2. For $\Lambda \approx 125$ TeV, which is the current limit from the Tevatron, BR ($\tilde{\chi}_1^0 \rightarrow \gamma \tilde{G}$) ≈ 0.91 . This will relax the limit on $m_{\tilde{\chi}_1^0}$ by a few GeV only. However, as the Tevatron experiments become sensitive to higher Λ , the value of BR ($\tilde{\chi}_1^0 \rightarrow \gamma \tilde{G}$) should be carefully folded into the calculation before extracting the $m_{\tilde{\chi}_1^0}$ limit. In the following we shall also consider more general GMSB models where the value of the BR is considerably smaller than unity and must be taken into account before extracting any limit from the Tevatron data.

BP I	BP II
$\Lambda=165$ TeV, $M_m = 2\Lambda$	$\Lambda=125$ TeV $M_m = 2\Lambda$
$\tan \beta=5$, $N_1 = N_2 = N_3 = 1$	$\tan \beta=20$, $N_1 = N_2 = N_3 = 1$
$m_h = 111.6$ GeV	$m_h = 114.8$ GeV

Table 3: Benchmark points in the minimal GMSB model.

In view of the above discussions we have chosen the points in Table 3 which are consistent with the constraints discussed above, for estimating the squark gluino contribution to the $\gamma - \gamma$ invariant mass distribution from di-photon + X events in the mGMSB model.

For point I with $\tan \beta = 5$, the computed m_h is consistent with the weaker bound and $\Lambda = \Lambda_{min}$ as obtained from Figure 2. This point yields gluino mass ($m_{\tilde{g}}$) = 1329 GeV and average squark mass ($m_{\tilde{q}}$) = 1725 GeV. For

Point II $\Lambda = \Lambda_{min}$ as obtained from the $m_{\tilde{\chi}_1^0}$ bound, since $\tan \beta = 20$. This leads to $m_{\tilde{g}} = 1035$ GeV and $m_{\tilde{q}} = 1334$ GeV. The squark-gluino contributions to the di-photon + X events in these scenarios will be computed in the next section.

In the mGMSB model a single scale (Λ) controls both the sfermion and gaugino masses. As a result these masses are of the same order. Over the years several extensions of the mGMSB models have been proposed. We shall collectively call them non-minimal models. For phenomenological studies such extensions can be realized by introducing new parameters in addition to the set of five parameters mentioned above.

One possibility is that the gaugino masses may be suppressed with respect to the sfermion masses [23]. This scenario can be studied by introducing a parameter $R (< 1)$ such that $\Lambda_G = R\Lambda_S$, where $\Lambda_G(\Lambda_S)$ is the scale in the gaugino (scalar) sector at the messenger scale.

More recently theoretically well-motivated extensions of the mGMSB model reflecting the above feature have been constructed. In a wide class of models the gaugino mass scale (Λ_G) happens to be severely suppressed in comparison to the sfermion mass scale (Λ_S)[24]. This suppression is a consequence of expanding around the lowest classical vacuum of the low energy effective theory [25]. This can be avoided, e.g., if the vacuum is an excited metastable state. It is, therefore, possible to construct gauge mediation models where the ratio of gaugino and sfermion masses continuously vary from very small to large values [26].

The sparticle spectra and BRs for different R can be computed by using, for example, online version of ISAJET. For $R < 1$ the gluino mass is expected to be significantly smaller than that in the mGMSB model ($R = 1$) with $\Lambda = \Lambda_S$. However, the chargino and the neutralino masses will also be correspondingly suppressed in the above model. Hence, the Tevatron bound does not allow arbitrarily small R as we shall see below.

For example, with $\Lambda_S = 124$, which corresponds to the Tevatron lower bound in the mGMSB model (see Point II), we obtain for $R = 0.6$, $m_{\tilde{\chi}_1^0} = 101$, $m_{\tilde{\chi}_2^0} = 205 \approx m_{\tilde{\chi}_1^\pm}$, $m_{\tilde{g}} = 667$ and $\text{BR}(\tilde{\chi}_1^0 \rightarrow \gamma \tilde{G}) = 0.98$. It is obvious that with such light electroweak gauginos, the combined electroweak gaugino production cross section at Tevatron is enhanced violating the bound. For $\tan \beta = 5$ (20) the modified bound turns out to be $\Lambda_S > 203(202)$ TeV. The Higgs masses in this two case are 112.7(117.5) GeV which is above the weaker m_h bound. Thus in contrast to the mGMSB model, the lower bound on Λ comes from the Tevatron data for both low and high $\tan \beta$. It is now easy to check the lower bounds on the gluino and average squark masses. They are $m_{\tilde{g}} \approx 1030$ GeV and $m_{\tilde{q}} \approx 2$ TeV. Thus although the minimum gluino mass is less than or comparable to the corresponding values in the mGMSB model, the average squark mass is much larger. Thus in general the size of the total squark-gluino signal and, consequently, the SUSY induced di-photon signal is expected to be smaller in non-minimal models with $R < 1$ compared to the corresponding mGMSB model.

It has further been pointed out that not only the overall mass scales in the gaugino and sfermion sectors may be different, the $SU(3)$, $SU(2)$ and $U(1)$ contributions of messenger fields to the masses of the gauginos and the

	BP III	BP IV	BP V	BP VI	BP VII	BP VIII
Masses	$\tan\beta=5$	$\tan\beta=20$	$\tan\beta=5$	$\tan\beta=20$	$\tan\beta=5$	$\tan\beta=20$
	$R_{st}=0.4$	$R_{st}=0.4$	$R_{st}=0.6$	$R_{st}=0.6$	$R_{st}=1$	$R_{st}=1$
	$\Lambda=160$	$\Lambda=170$	$\Lambda=145$	$\Lambda=138$	$\Lambda=132$	$\Lambda=96$
	$N_1=N_2=2,$ $N_3=1$	$N_1=N_2=2,$ $N_3=1$	$N_1=N_2=2,$ $N_3=1$	$N_1=N_2=2,$ $N_3=1$	$N_1=N_2=2,$ $N_3=1$	$N_1=N_2=2,$ $N_3=1$
$m_{\tilde{g}}$	601.43	634.84	769.25	735.97	1080.68	811.35
$m_{\tilde{u}_L}$	1707.57	1807.49	1576.26	1505.46	1512.87	1125.34
$m_{\tilde{u}_R}$	1548.76	1637.86	1432.95	1368.84	1382.82	1032.09
$m_{\tilde{d}_L}$	1709.33	1809.28	1578.16	1507.62	1514.84	1128.21
$m_{\tilde{d}_R}$	1532.50	1620.46	1418.62	1355.44	1370.62	1023.95
$m_{\tilde{b}_1}$	1543.42	1617.90	1427.69	1352.12	1377.27	1019.73
$m_{\tilde{b}_2}$	1636.31	1728.66	1511.61	1440.96	1454.46	1080.55
$m_{\tilde{\tau}_1}$	1380.99	1468.53	1280.93	1231.20	1245.24	937.82
$m_{\tilde{\tau}_2}$	1649.96	1742.71	1525.31	1454.71	1468.71	1095.36
$m_{\tilde{\nu}_e}$	779.80	829.17	715.96	682.56	679.52	494.71
$m_{\tilde{e}_L}$	789.04	838.58	725.12	691.94	688.63	504.75
$m_{\tilde{e}_R}$	389.25	414.11	355.88	339.15	332.85	243.13
$m_{\tilde{\nu}_\tau}$	779.64	826.54	715.82	680.40	679.39	493.20
$m_{\tilde{\nu}_1}$	388.55	399.75	355.00	327.04	331.61	234.25
$m_{\tilde{\nu}_2}$	788.82	835.52	724.92	689.48	688.44	503.11
$m_{\tilde{\chi}_1^0}$	-174.37	-185.26	-236.53	-221.43	-332.55	-216.57
$m_{\tilde{\chi}_2^0}$	-332.91	-325.56	-377.98	-309.82	372.92	249.46
$m_{\tilde{\chi}_3^0}$	441.64	375.01	406.32	323.65	-398.81	-286.55
$m_{\tilde{\chi}_4^0}$	-477.58	-441.27	-524.44	-490.80	-744.13	-549.85
$m_{\tilde{\chi}_1^\pm}$	-325.08	-320.00	-369.82	-304.86	-366.79	-240.69
$m_{\tilde{\chi}_2^\pm}$	-481.08	-443.14	-524.45	-484.62	-735.66	-543.03
m_h	111.38	116.65	111.01	115.70	111.02	114.06
m_H	908.35	860.75	832.37	711.81	778.70	516.90
m_A	907.39	860.54	831.35	711.61	777.63	516.72
m_{H^\pm}	911.02	864.64	835.29	716.49	781.82	523.31

Table 4: Spectra for benchmark points in different non-minimal GMSB scenarios.

sfermions having different gauge quantum numbers, may also differ from each other. This happens, e.g, when the messenger fields do not belong to a complete multiplet of a GUT group (say, $SU(5)$) [23].

Let us concentrate on a phenomenological model characterized by 5 parameters in addition to M , $\tan \beta$ and $\text{sign}(\mu)$: R (defined above), Λ_S , N_1 , N_2 and N_3 . In the limit $R = 1$ and $N_1 = N_2 = N_3 = N$, this model reduces to mGMSB. The explicit mass formulae for the sfermions and the gauginos and further references can be found in Appendix A of [23].

The sparticle spectrum in this model can be computed by ISAJET. The Bino, Wino and gluino masses at the messenger scale are proportional to N_1, N_2 and N_3 respectively. Clearly if $N_1, N_2 > N_3$, the mass difference

between the electroweak gauginos and gluinos at the electroweak scale obtained by renormalization group evolution, will be reduced. Thus in this scenario the Tevatron bound becomes compatible with relatively light gluinos and, hence, one obtains a larger number of SUSY induced di-photon events. We illustrate some representative sparticle spectra with several benchmark points (BP III - BP VIII) in Table 4.

For each point in Table 4 the dominant chargino-neutralino pair production cross section (NLO) as a function of Λ is computed with PROSPINO assuming $m_{\tilde{\chi}_1^\pm} \approx m_{\tilde{\chi}_2^0}$. The K-factors for some representative values of $m_{\tilde{\chi}_1^\pm}$ are given in Table 5. Comparing the computed value with the the cross section upper bound from Tevatron data, we obtain Λ_{min} in each case. Each Λ_S presented in Table 4 is above the corresponding Λ_{min} .

$m_{\tilde{\chi}_1^\pm}$	K- factor
100	1.39
200	1.29
300	1.15
400	0.99

Table 5: The K factors of $\chi_1^+ \chi_2^0$ production at the Tevatron for different $m_{\tilde{\chi}_1^\pm}$. We choose mass of the final state as the QCD scale.

It may be noted from Table 4 that for most of the non-minimal models of this type, the gluino masses are significantly smaller than one TeV. Another point of phenomenological interest is the composition of the electroweak gauginos. In the non-minimal model μ as determined by the electroweak symmetry breaking condition often turns out to be comparable or even smaller than M_1 . As a result the higgsino component of the NLSP changes significantly. In Table 6 we present M_1, M_2 and μ in each model. The BR ($\tilde{\chi}_1^0 \rightarrow \gamma \tilde{G}$) is also shown. It follows that whenever the NLSP develops a significant higgsino component, channels like $\tilde{\chi}_1^0 \rightarrow Z \tilde{G}, \tilde{\chi}_1^0 \rightarrow h \tilde{G}$ open up and BR ($\tilde{\chi}_1^0 \rightarrow \gamma \tilde{G}$) decreases. This has been carefully taken into account in extracting limits from the Tevatron data as well as in computing the size of the di-photon signal at the LHC in different scenarios.

General gauge mediated symmetry breaking (GGMSB) models have been proposed recently [27]. These theoretically well-motivated models incorporate the features of the above phenomenological models. A large number of authors have recently studied the phenomenology of GGMSB [28]. In such a general framework, all gaugino mass parameters are independent of each other and squark masses and gluino mass are not correlated. Thus squark masses can be lighter in contrast to the models discussed above. To illustrate this point, we take two benchmark points where squark masses are free parameters. In BP IX, we take the point BP III and set all squark masses to be 1 TeV. The BP X point is identical to BP V with $m_{\tilde{q}} = m_{\tilde{g}}$.

The total SUSY cross section at the LHC in each scenario is also presented in Table 6. The leading order and

Points	$M_{\tilde{q}}$	$M_{\tilde{g}}$	M_1	M_2	μ	Total NLO cross sec	$\text{Br}(\chi_1 \rightarrow \gamma + \tilde{G})$	Effective cr-sec
BP I	1725	1329	240	445	884	221 fb (19 fb)	0.85	160 fb (14 fb)
BP II	1334	1035	181	339	502	1.1 pb (84 fb)	0.91	910 fb (70 fb)
BP III	1618	601	181	349	432	10.5 pb (583 fb)	0.89	8.3 pb (462 fb)
BP IV	1509	635	192	371	363	8.7 pb (414 fb)	0.87	6.6 pb (313 fb)
BP V	1495	769	247	474	397	3.0 pb (112 fb)	0.81	2.0 pb (74 fb)
BP VI	1427	736	235	452	313	4.1 pb (207 fb)	0.79	2.6 pb (129 fb)
BP VII	1439	1081	376	718	364	725 fb (48 fb)	0.38	105 fb (7 fb)
BP VIII	1072	811	273	525	240	4.8 pb (319 fb)	0.35	590 fb (39 fb)
BP IX	1000	601	181	349	432	16.8 pb (822 fb)	0.89	13.3 pb (651 fb)
BP X	770	770	247	474	397	11.0 pb (640 fb)	0.81	7.2 pb (420 fb)

Table 6: *The average squark mass, gluino mass, total NLO SUSY production cross section at the LHC for $\sqrt{s}=14$ TeV (7 TeV) and $\text{BR}(\chi_1 \rightarrow \gamma + \tilde{G})$ for benchmark points (BP I to BP X). The electroweak gaugino mass parameters M_1 , M_2 and μ are also given . Note that in case of BP I, BP II and BP VII, the EW gaugino production cross sections are comparable to the strong production cross sections.*

next to leading order (NLO) squark gluino cross sections are computed by PROSPINO [19]. The relatively modest electroweak production cross sections are computed by PYTHIA and multiplied by the appropriate K factor, as discussed above. In each case the QCD scale is chosen to be equal to the mass or the average mass of the sparticles in the final state and CTEQ 5L and CTEQ 5M parton density functions have been used for LO and NLO cross sections respectively. The cross sections agree well with ref [29].

It is found that the scenarios with relatively light gluinos (BP III - VI) have significantly larger cross sections compared to the representative mGMSB scenarios (BP I and BP II). However, for $R = 1$, (BP VII and BP VIII) the NLSP has substantial higgsino component. As a result the relevant BRs are also small in the corresponding models and, consequently, the number of the SUSY di-photon events is rather small as we shall see in the next section.

Recently the CMS collaboration has reported negative results for squark-gluino search [30] search in the di-photon + \cancel{E}_T channel in the context of a simplified GGMSB model [31]. In this model the $m_{\tilde{\chi}_1^0}$ (the NLSP mass), $M_{\tilde{q}}$ and $M_{\tilde{g}}$ at the weak scale are taken as variables whereas all other sparticle masses are fixed at 1.5 TeV. The impact of the squark-gluino induced di-photons in this case on the $\gamma\gamma$ invariant mass data collected by dedicated Higgs search experiments in the context of this model will also be reported in the next section.

3 Footprints of squark-gluino events in the di-photon invariant mass data collected by the Higgs search experiments at the LHC.

From the sparticle spectra presented in the last section we find that in all cases the pseudoscalar Higgs boson mass (M_A) is much larger than M_Z . Hence we are in the deep decoupling regime. As a result the production cross sections and the BRs of the h-boson are practically the same as the SM Higgs boson having the same mass. For h-bosons with masses a few GeV above the LEP lower bound, the di-photon+ X channel is the most promising signal.

As already mentioned in the introduction the prospect of discovering the h-signal in the di-photon+ X channel at the LHC, is not the main concern of this paper. This has been dealt with in great depth by the LHC collaborations [6, 7]. Our main task is to study the possibility of distortion in the tail of the $\gamma - \gamma$ invariant mass distributions in different GMSB scenarios in typical Higgs search experiments. For this we simulate by PYTHIA the SM backgrounds and squark-gluino events in the models discussed in Section 2 using the cuts employed by Higgs search experiments.

We begin by following the standard selection procedures for Higgs search in the di-photon + X channel by the CMS collaboration [6] at 14 TeV. We note that ATLAS collaboration [32] has used same cuts both for 7 and 14 TeV analyses. Thus our approach seems to be reasonable.

We require events with exactly two isolated photons with pseudo-rapidity $|\eta| < 2.5$ and p_T greater than 40 GeV and 35 GeV respectively. We put the following isolation conditions on photons.

1. No charged particles with p_T larger than 1.5 GeV/c should be present inside a cone with $\Delta R < 0.3$ around the photon candidate where $\Delta R = \sqrt{\Delta\eta^2 + \Delta\phi^2}$.
2. The total E_T of electrons or photons with $0.06 < \Delta R < 0.35$ around the direction of the selected photon candidate, must be less than 6 GeV in the barrel and 3 GeV in the endcaps.
3. The total transverse energies of hadrons within $\Delta R < 0.3$ around the photon candidate must be less than 6 GeV in the barrel and 5 GeV in the endcaps.

The irreducible SM backgrounds are from i) $q \bar{q} \rightarrow \gamma \gamma$ and ii) $g g \rightarrow \gamma \gamma$ events. We generate these backgrounds by PYTHIA 6.4.21 subject to the above cuts. The LO cross sections of the backgrounds are computed by PYTHIA. The K factors of these two processes are given in [6] for 14 TeV LHC(1.5 and 1.2 respectively). The NLO cross sections for the SM backgrounds at 7 TeV are not available in the literature. As a reasonable guess we take the same K factor for i) and (ii) to be 1.5 and 1.2.

The additional cuts related to photon reconstruction employed by the CMS collaboration cannot be implemented in our analysis with the toy detector of PYTHIA. We assume that their absence will affect the SUSY events and the background similarly and our main conclusions will be by and large valid. We have also ignored the instrumental backgrounds. We admit that the main purpose of this analysis is to illustrate the possibility of distortion in the shape of an expected distribution due to new physics and not to present very accurate numerical results.

The sparticle spectra in different non-minimal models (BP III - VIII in Table 4) can be readily generated by online ISAJET [13]. The spectra in mGMSB (BP I and II in Table 3) and GGMSB models (BP IX and X) have been generated by SUSYHIT [34]. Finally the spectra are interfaced with PYTHIA for event generation. For squark-gluino events the NLO cross sections are directly computed by PROSPINO (see section 2).

Processes	$M_{\gamma\gamma} > 200$	$M_{\gamma\gamma} > 300$	$M_{\gamma\gamma} > 400$	$M_{\gamma\gamma} > 500$	$M_{\gamma\gamma} > 600$
Born (SM bg)	707.6	219.5	91.3	42.8	20.6
Box (SM bg)	78.9	12.8	2.5	0.6	0.1
BP I	5.5	3.0	1.5	0.7	0.3
BP II	18.2	7.7	3.1	1.3	0.6
BP III	106.6	44.8	17.7	6.9	2.8
BP IV	75.7	32.0	12.7	5.0	2.1
BP V	23.8	12.2	5.6	2.5	1.1
BP VI	38.4	17.7	7.3	3.0	1.2
BP VII	0.2	0.1	0.1	0.0	0.0
BP VIII	13.4	6.1	2.6	1.1	0.5
BP IX	134.5	56.2	22.0	8.6	3.3
BP X	128.9	71.5	36.0	17.7	8.6

Table 7: Number of events for $\mathcal{L} = 1 \text{ fb}^{-1}$ in different invariant mass bins in benchmark scenarios presented in Table 6. We consider bins with $M_{\gamma\gamma} > 200 \text{ GeV}$ or more at LHC 7 TeV run.

We next compute invariant mass distribution of the di-photons from h-decays, the squark-gluino events and the SM backgrounds. We show in Table 7 the total number of events in all bins with $M_{\gamma\gamma} \geq 200, 300, 400, 500$ and 600 GeV for different benchmark points for $\mathcal{L} = 1 \text{ fb}^{-1}$. We have checked that the number of events from the Higgs signal in these bins are indeed negligible but sizable contributions come from the other two sources. It is interesting to note that the contribution from the squark-gluino events are statistically significant in some cases. For example, the total number of background events (B) in all bins with $M_{\gamma\gamma} \geq 300$ for $\mathcal{L} = 2 \text{ fb}^{-1}$ is 464. The corresponding number of squark-gluino induced events (S) for in BP X is 143. Hence $S/\sqrt{B} = 6.64$ in this case. Similarly for BP IX the contribution from squark-gluino production is above 5σ fluctuation of the expected SM background. The number of events for BP III and IV are also reasonably large albeit with smaller significance at this \mathcal{L} .

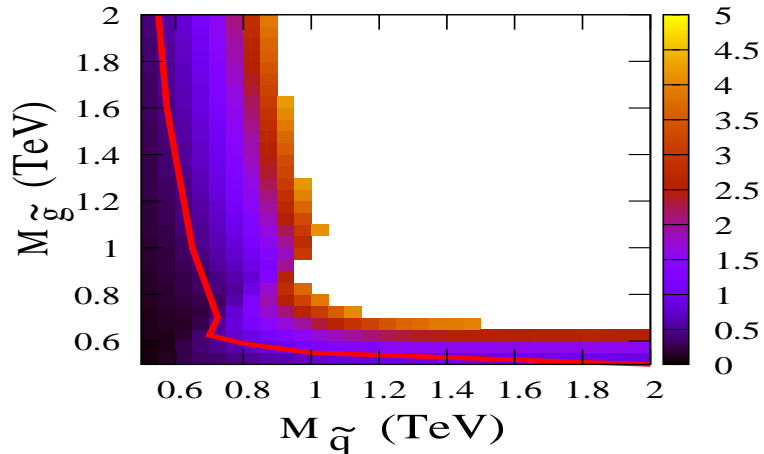


Figure 4: *The parameter space in a simplified GGMSB model (the coloured region) where the distortion in the tail of the $\gamma - \gamma$ invariant mass distribution is observable at the ongoing LHC experiments with $\mathcal{L} \leq 5 \text{ fb}^{-1}$ (see text for the details). The parameter space below the red line has already been ruled out by the CMS collaboration [30].*

Of course such a small integrated luminosity is insufficient for Higgs discovery via the di-photon + X channel at the on going LHC experiments [35]. However, it is encouraging to note that even at this low \mathcal{L} , BSM physics can show up in the distorted tail of the $\gamma - \gamma$ invariant mass distribution. Moreover, if observed, this would certainly disfavour the competing SUSY breaking models like mSUGRA which do not have natural sources of such di-photons . This observation would also disfavour a two Higgs doublet extension of the SM model with comparable h- mass and couplings. Such a model may predict the Higgs peak at the right place but not the appreciable distortion of the tail. appreciably.

It may also be noted that the contribution of the mGMSB is negligible for values of Λ constrained by the Tevatron data. In contrast, some of the non-minimal scenarios contribute significantly. Moreover, for $R = 1$, the SUSY contributions even in non-minimal scenarios are negligible. Thus if a distortion of the tail is indeed observed it may indicate a non-minimal model with $R < 1$.

Mh (GeV)	$gg \rightarrow h$ NLO (pb)	Vector Boson Fusion NLO (pb)	$Wh, Zh, t\bar{t}h$ NLO (pb)	Br(h $\rightarrow \gamma\gamma$)
115	39.2	4.7	3.8	0.00208

Table 8: *Higgs production cross-sections in the SM at the LHC for $\sqrt{s}=14$ TeV and the branching ratio to the di-photon final state(taken from CMS TDR).*

We next consider the simplified GGMSB model studied by the CMS collaboration [30], briefly discussed at the end of section 3. We fix $m_{\tilde{\chi}_1^0}$ at 50 GeV. The di-photons originating from the squark-gluino events are studied for different combinations of the common squark mass $M_{\tilde{q}}$ and the gluino mass $M_{\tilde{g}}$. The results are presented in Figure 4. The coloured area corresponds to the region where S/\sqrt{B} as defined above is ≥ 5 for an integrated luminosity determined by the colour codes given on the vertical line next to the figure. In computing the significance we have considered the events accumulated in all bins with $M_{\gamma\gamma} > 300$. The parameter space already excluded by the CMS collaboration [30] from the $\mathcal{L} = 36 \text{ fb}^{-1}$ data is shown by the region below the red line. Thus hints of GGMSB scenarios can be obtained for a fairly large parameter space.

We next repeat the above analysis for experiments at LHC - 14 TeV. The cross sections in Table 8 are from the CMS TDR [6], Table 2.1 for $m_h = 115 \text{ GeV}$ at a proton-proton center-of-mass energy of $\sqrt{s}=14 \text{ TeV}$. The NLO cross sections of the dominant SM backgrounds are also taken from [6].

The irreducible SM backgrounds discussed before and the di-photon events stemming from squark-gluino events in different GMSB models are generated by PYTHIA.

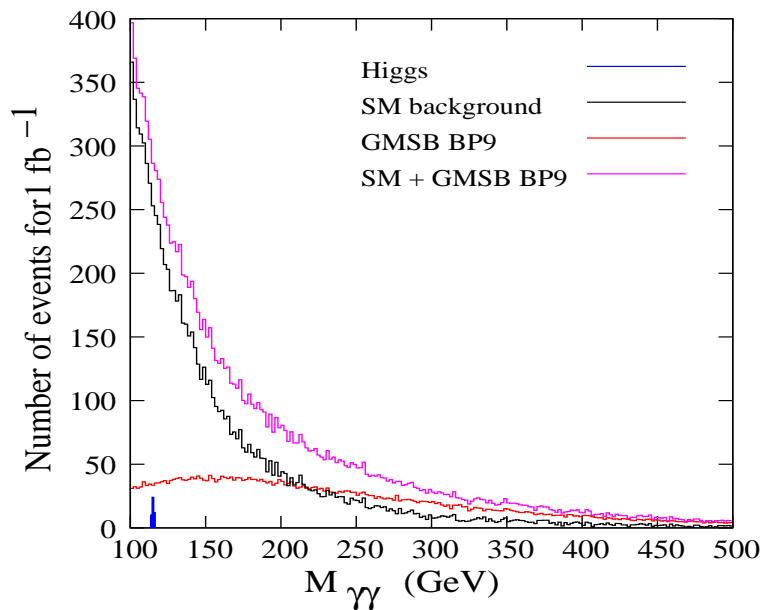


Figure 5: *The di-photon invariant mass distribution for the SM backgrounds, the Higgs signal ($m_h = 115 \text{ GeV}$) and squark-gluino events for the GGMSB benchmark point BP IX at the LHC-14 TeV run with $\mathcal{L} = 1 \text{ fb}^{-1}$.*

We present in Figure 5 the distribution of $M_{\gamma\gamma}$ from the decay of a Higgs with $m_h=115 \text{ GeV}$ (the tiny blue histogram), the SM backgrounds (the black histogram) and the squark-gluino events from BP IX (the red histogram) for $\mathcal{L} = 1 \text{ fb}^{-1}$ at 14 TeV center-of-mass energy. The combined distribution of the SM backgrounds and the SUSY events is also shown (the purple histogram). It is found that the SM background falls off rapidly

Processes	$M_{\gamma\gamma} > 200$	$M_{\gamma\gamma} > 400$	$M_{\gamma\gamma} > 600$	$M_{\gamma\gamma} > 1000$
Born (SM bg)	1275	185	54	8
Box (SM bg)	302	15	1	0
BP I	54	21	7	1
BP II	214	60	18	2
BP III	1876	434	98	7
BP IV	1519	358	82	6
BP V	547	177	51	5
BP VI	621	173	42	4
BP VII	2	1	1	0
BP VIII	157	45	12	1
BP IX	2580	551	112	7
BP X	1977	653	199	22

Table 9: Number of events for $\mathcal{L} = 1 \text{ fb}^{-1}$ in the invariant mass bins starting from $M_{\gamma\gamma} > 200$ GeV at the LHC 14 TeV run.

for higher values of the invariant mass. Whereas, the SUSY contribution is fairly constant for a significant part of that region. The distribution of events in different bins is shown in Table 9.

On the basis of the earlier simulations [6] one does not expect a statistically significant Higgs signal at this tiny \mathcal{L} . Yet the distortion of the distribution far away from the Higgs peak is already worth noting. For example, the number (S) of the squark-gluino induced events for $M_{\gamma\gamma} \geq 400$ GeV turns out to be 551. The corresponding number (B) for the SM background is 200. Thus S / \sqrt{B} , as defined above is 39. This suggests that the excess of events coming from sparticle production, if observed near the tail of the distribution, can not be dismissed as mere statistical fluctuation. The number of events with $M_{\gamma\gamma} \geq 200$ GeV or more for other benchmark points are given in Table 9.

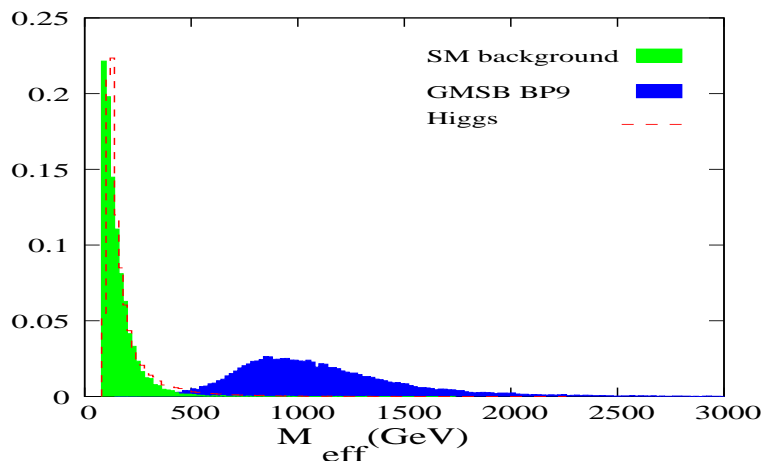


Figure 6: Normalized effective mass distribution of the Higgs signal (Red dotted line), the GMSB benchmark point BP IX (blue) and the SM di-photon background (green).

The presence of squark gluino events may be revealed by other distributions as well. We present in Figure 6 the effective mass distribution of the Higgs signal, the SM background and the SUSY events for BP IX for $\mathcal{L} = 1 \text{ fb}^{-1}$ at 14 TeV. We have defined the effective mass M_{eff} as the scalar sum of jet p_T 's, lepton p_T 's, photon p_T 's and missing transverse momentum:

$$M_{eff} = \sum_{jet} p_T + \sum_{lepton} p_T + \sum_{photon} p_T + \cancel{p}_T. \quad (1)$$

The peak of the distribution at a high M_{eff} strongly indicate some BSM physics with new heavy particles and disfavour models with an extended Higgs sector but no new heavy particles.

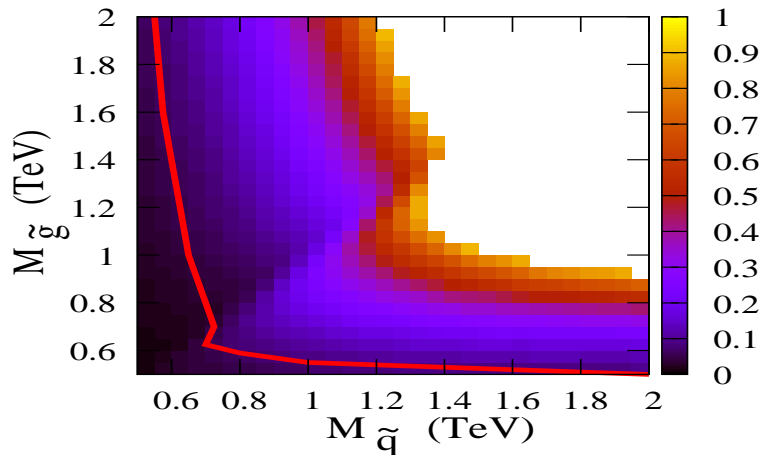


Figure 7: Same as Figure 4 but for LHC experiments at 14 TeV with $\mathcal{L} \leq 1 \text{ fb}^{-1}$.

In Fig 7 we present our results for the simplified model [30]. The conventions are the same as in Figure 4 except that we focus on the distortion of the $M_{\gamma-\gamma}$ distribution for $\mathcal{L} \leq 1 \text{ fb}^{-1}$ which will be accumulated at a very early stage of experiments at 14 TeV. A large region of the parameter space may indicate the distortion looked for.

A few di-photon events resulting from sparticle production in some GGMSB model may enter into the Higgs peak. In Table 10 we present the di-photon + X events in the neighbourhood of the Higgs peak at 115 for different scenarios for $\mathcal{L} = 1 \text{ fb}^{-1}$ at 14 TeV. In a bin of $m_h \pm 1.4$, as suggested in [7], we find the number of genuine Higgs induced events to be 43. The SUSY contributions to the same region are 33, 24, 47 and 19 for BP III, BP IV, BP IX and BP X respectively. Thus the presence of SUSY events is indeed significant.

Of course a suitable cut can easily eliminate these unwanted events. For example, the distribution in Figure 6 suggests that a cut of $M_{eff} < 300$ can eliminate the SUSY contributions around the Higgs mass peak, while the Higgs signal and the SM backgrounds remain practically unaffected. Before the cut, however, the non-standard origin of the Higgs boson will be revealed by the M_{eff} distribution. The SUSY events around the Higgs peak can also be eliminated by putting an upper cut on the \cancel{E}_T . However, as already discussed the M_{eff} distribution

Processes	109	110	111	112	113	114	115	116	117
Born (SM bg)	90	87	83	82	81	85	76	72	67
Box (SM bg)	66	66	60	59	57	54	57	49	50
BP I	0.2	0.2	0.2	0.2	0.2	0.2	0.2	0.2	0.2
BP II	1.2	1.2	1.1	1.2	1.2	1.3	1.2	1.2	1.1
BP III	10.6	11.4	11.9	11.7	11.1	12.2	11.8	11.5	11.3
BP IV	8.1	8.1	8.7	8.1	8.1	8.8	9.0	8.4	8.8
BP V	1.8	1.9	1.9	2.1	1.9	2.0	1.6	2.0	2.1
BP VI	2.1	2.6	2.7	2.7	2.8	2.3	2.7	3.4	2.5
BP VII	0.0	0.0	0.2	0.0	0.0	0.0	0.0	0.0	0.0
BP VIII	0.6	0.8	0.8	0.7	0.8	2.7	0.5	0.6	0.9
BP IX	16.6	19.6	16.5	16.8	17.1	17.6	16.8	17.1	17.5
BP X	6.0	6.5	6.3	6.1	6.8	6.7	6.5	6.5	6.9

Table 10: Number of events in the invariant mass bins 109 to 117 GeV from different sources after all cuts for $\mathcal{L} = 1 \text{ fb}^{-1}$ at the 14 TeV run. The total Higgs cross section after passing all cuts is around 43 fb leading to 43 events at 1 fb^{-1} distributed in 114-116 GeV bins.

provides a strong hint for the presence of new heavy particles, whereas large \cancel{E}_T can come from massless particles and/or jet energy mis-measurements.

4 Conclusion

In this paper we analyze the invariant mass distribution of the di-photons to be minutely studied by the dedicated Higgs search experiments in the di-photon + X channel at the LHC. In the SM only a tiny peak at m_h above the SM background is expected. In GMSB models, in contrast, the di-photons stemming from squark-gluino events may distort the tail of the distribution far away from the Higgs mass peak revealing the non-standard origin of the Higgs boson. In this paper we explore this possibility both at LHC 7 TeV and 14 TeV experiments by considering benchmark points in different GMSB models - minimal as well as non-minimal (Table 5) [10, 11, 23, 24, 25, 26, 27]. We also consider a simplified model recently employed by the CMS collaboration to interpret their negative results for SUSY search in the GGMSB models and illustrate the above point through a detailed parameter space scan.

We first consider the minimal GMSB [10, 11] model subject to the lower bounds on m_h from LEP and on the lightest neutralino (NLSP) mass (or equivalently on the scale Λ) from Tevatron (see Figures 1 and 2). The resulting lower bounds on the squark-gluino masses are so strong that di-photon events induced by sparticle production with tiny cross-sections are unlikely to affect the h-signal. This has been illustrated with the help of two benchmark points (BP I and II, Table 3) in section 3.

The $D\mathcal{O}$ and the CDF experiments actually constrain quantity $\sigma_{SUSY} \times BR(\tilde{\chi}_1^0 \rightarrow \gamma \tilde{G})^2$, where σ_{SUSY} is the total sparticle production cross section within the kinematic reach of the Tevatron, $BR(\tilde{\chi}_1^0 \rightarrow \gamma \tilde{G})$ is the branching ratio underlying each single photon event. The bounds on Λ or the NLSP mass in the mGMSB model are derived with the assumption that the above BR is one.

If $BR(\tilde{\chi}_1^0 \rightarrow \gamma \tilde{G})^2$ is significantly smaller than 1, the limit on σ_{SUSY} and, consequently, on Λ or the NLSP mass become weaker. This can happen in the mGMSB model (Table 2) and, more importantly, in its generalizations (Table 6). While extracting Λ_{min} from the Tevatron data in different models we have taken this possible reduction into account and have selected our benchmark points accordingly (see Table 4). In some of the models the total squark-gluino cross sections are significantly larger than the expected values in the mGMSB model and the relevant BRs are not too small either (see Table 6). More recently it has been shown that the distinct features of these phenomenological models can be incorporated into theoretically well-motivated models[24, 25, 26, 27].

Our main results are as follows:

1. The di-photon + X events from sparticle production may change the shape of the tail of the $\gamma - \gamma$ invariant mass distributions which will be analyzed with utmost care by the LHC experiments. This distortion was shown to be statistically significant in several benchmark scenarios of the non-minimal GMSB models for both LHC 7 TeV (Table 7) and 14 TeV (Table 9) experiments. In both cases the traces of new physics beyond the Higgs sector may show up at the early stages of the experiments with \mathcal{L} insufficient for the discovery of the h boson in the di-photon + X channel. Similar conclusions follow by analyzing a simplified model [30] (Figures 4 and 7).
2. Other observables like the effective mass distribution of the di-photon events may also contain hints of new physics consisting of heavy particles (Figure 6). Unexpected shapes of this distribution may disfavour not only the SM but i) extensions of it with larger Higgs sectors but no new heavy particles, ii) models with other SUSY breaking mechanisms like mSUGRA which do not have natural sources of di-photon events from sparticle production and iii) the mGMSB model subject to the constraints from LEP and Tevatron.
3. The squark-gluino induced $\gamma - \gamma$ events may contaminate the peak of the invariant mass distribution at m_h (see Table 10). To improve the purity of the h-signal one may implement cuts on suitable kinematical variables like an upper cut on the effective mass (see Figure 6) or an upper cut on the missing energy which eliminate the sparticle induced events in the Higgs peak.

References

- [1] L. Susskind, Phys. Rev. D **20**, 2619 (1979); G. 't Hooft in *Recent Developments in Gauge Theories*, Proceedings of the Cargèse Summer Institute, Cargèse, France, eds. G. 't Hooft *et al.* ; M. Veltman, Acta. Phys. Pol. **12**, 437 (1981).
- [2] E. Gildener and S. Weinberg, Phys. Rev. D **13**, 3333 (1976); E. Gildener, Phys. Rev. D **14**, 1667 (1976).
- [3] LEP Electroweak Working Group, <http://lepewwg.web.cern.ch>.
- [4] H. P. Nilles, Phys. Rept. **110**, 1 (1984); H. E. Haber and G. L. Kane, Phys. Rept. **117**, 75 (1985); S. P. Martin, arXiv:hep-ph/9709356; M. Dress, R. M. Godbole, and P. Roy, Theory and Phenomenology of Sparticles (World Scientific, Singapore, 2005).
- [5] For a review see, e.g., A. Djouadi, Phys. Rept. **459**, 1 (2008) [arXiv:hep-ph/0503173].
- [6] G. L. Bayatian *et al.* [CMS Collaboration], J. Phys. G **34** (2007) 995.
- [7] ATLAS collaboration: CERN-OPEN-2008-020, 2008.
- [8] N. Bhattacharyya, Amitava Datta, M. Guchait, M. Maity and S. Poddar, Phys. Rev. D **82**, 035022 (2010).
- [9] R. Arnowitt, A. H. Chamseddine and P. Nath, Phys. Rev. Lett. **49**, 970 (1982); R. Barbieri, S. Ferrara and C. A. Savoy, Phys. Lett. B **119**, 343 (1982); L. J. Hall, J. Lykken and S. Weinberg, Phys. Rev. D **27**, 2359 (1983); P. Nath, R. Arnowitt and A. H. Chamseddine, Nucl. Phys. B **227**, 121 (1983); N. Ohta, Prog. Theor. Phys. **70**, 542 (1983).
- [10] P. Fayet, Phys. Lett. **B70**, 461 (1977); M. Dine, W. Fischler and M. Srednicki, Nucl. Phys. B **189**, 575 (1981); S. Dimopoulos and S. Raby, Nucl. Phys. B **192**, 353 (1981); M. Dine and A. Nelson, Phys. Rev. D **48**, 1277 (1993); M. Dine, A. E. Nelson, Y. Shirman, Phys. Rev. **D51**, 1362-1370 (1995); M. Dine, A. E. Nelson, Y. Nir and Y. Shirman, Phys. Rev. D **53**, 2658 (1996). S. Dimopoulos, S. D. Thomas, J. D. Wells, Nucl. Phys. **B488**, 39-91 (1997).
- [11] For reviews and a more complete list of references see, e.g., G. F. Giudice and R. Rattazzi, Phys. Rep. **322**, 419 (1999).
- [12] A. Djouadi, J. L. Kneur and G. Moultaka, Comput. Phys. Commun. **176**, 426 (2007).
- [13] F. E. Paige, S. D. Protopopescu, H. Baer and X. Tata, arXiv:hep-ph/0312045. For online version see <http://www.phys.ufl.edu/~jblender/isajet/isajet.html>
- [14] J. A. Bagger, K. T. Matchev, D. M. Pierce, R. -j. Zhang, Phys. Rev. **D55**, 3188-3200 (1997); H. Baer, M. Brhlik, C. -h. Chen, X. Tata, Phys. Rev. **D55**, 4463-4474 (1997); H. Baer, P. G. Mercadante, X. Tata,

- Y. -l. Wang, Phys. Rev. **D60**, 055001 (1999); J. L. Diaz-Cruz, D. K. Ghosh, S. Moretti, Phys. Rev. **D68**, 014019 (2003).
- [15] R. Barate *et al.* [LEP Working Group for Higgs boson searches and ALEPH and DELPHI and L3 and OPAL Collaborations], Phys. Lett. **B565**, 61-75 (2003).
- [16] S. Heinemeyer, W. Hollik and G. Weiglein, Phys. Rep. **425**, 265 (2006), S. Heinemeyer, Int. J. Mod. Phys. A **21**, 2659 (2006).
- [17] V. M. Abazov *et al.* [D0 Collaboration], Phys. Rev. Lett. **105**, 221802 (2010).
- [18] T. Sjostrand, S. Mrenna and P. Z. Skands, JHEP **0605**, 026 (2006) [arXiv:hep-ph/0603175].
- [19] W. Beenakker, R. Hopker and M. Spira, arXiv:hep-ph/9611232. Please see See <http://www.thphys.uni-heidelberg.de/plehn/prospino/> or <http://people.web.psi.ch/spira/prospino/>
- [20] W. Beenakker, M. Klasen, M. Kramer, T. Plehn, M. Spira and P. M. Zerwas, Phys. Rev. Lett. **83**, 3780 (1999) [Erratum-ibid. **100**, 029901 (2008)].
- [21] CDF Collaboration: CDF/PUB/CDFR/PUBLIC/9625, 2008.
- [22] CDF Collaboration: CDF note 10202,2010.
- [23] For a review and further references see, e.g., R. Culbertson *et al.*, hep-ph/0008070.
- [24] K. I. Izawa, Y. Nomura, K. Tobe and Y. Yanagida, Phys. Rev. D **56**, 2886 (1997); R. Kitano, H. Ooguri and Y. Ookouchi, Phys. Rev. D **75**, 045022 (2007); C. Csaki, Y. Shirman and J. Terning, J. High Energy Phys. **0705**, 099 (2007); S. Abel, C. Durnford, J. Jaeckel and V. V. Khoze, Phys. Lett. B **661**, 201 (2008).
- [25] Z. Komargodski and D. Shih, J. High Energy Phys. **0904**, 093 (2009).
- [26] S. A. Abel, J. Jaeckel and V. V. Khoze, Phys. Lett. B **682**, 441 (2010).
- [27] P. Meade, N. Seiberg and D. Shih, Prog.Theor.Phys.Suppl. 177,143 (2009); M. Buican, P. Meade, N. Seiberg and D. Shih, J. High Energy Phys. **0903**, 067 (2009).
- [28] L. M. Carpenter, arXiv:0812.2051 (hep-ph); A. Rajaraman, Y. Shirman, J. Smidt and F. Yu, Phys. Lett. B **678**, 367 (2009); J. D. Mason, D. E. Morrissey, D. Poland, Phys. Rev. **D80**, 115015 (2009); P. Meade, M. Reece, D. Shih, J. High Energy Phys. **1005**, 105 (2010), J. High Energy Phys. **1010**, 067 (2010); J. T. Ruderman and D. Shih, J. High Energy Phys. **1011**, 046 (2010); S. A. Abel, M. J. Dolan, J. Jaeckel and V. V. Khoze, J. High Energy Phys. **0912**, 001 (2009); R. Sato and S. Shirai, Phys. Lett. B **692**, 126 (2010); J. Jaeckel, V. V. Khoze and C. Wymant, JHEP **1104**, 126 (2011); S. Biswas, J. Chakraborty and S. Roy, arXiv:1010.0949 [hep-ph]; T. Ruderman and D. Shih, arXiv:1103.6083; M. J. Dolan, D. Grellscheid, J. Jaeckel, V. V. Khoze, P. Richardson, [arXiv:1104.0585 [hep-ph]].

- [29] W. Beenakker, S. Brensing, M. Kramer, A. Kulesza, E. Laenen and I. Niessen, *JHEP* **0912**, 041 (2009).
- [30] CMS collaboration, arXiv:1103.0953 (hep-ex)
- [31] LHC New Physics Working Group, "Simplified Models for LHC New Physics Searches", June 2010.
- [32] ATLAS collaboration, ATLAS-CONF-2011-025, 2011.
- [33] photon isolation by cms.
- [34] A. Djouadi, M. M. Muhlleitner and M. Spira, *Acta Phys. Polon. B* **38**, 635 (2007).
- [35] see,e.g., the talk by V.Sharma at XLVI Rencontres De Moriond (2011).

